

Observation of a Magnetically Induced Wigner Solid

E. Y. Andrei,^(a) G. Deville, D. C. Glattli, and F. I. B. Williams

Service de Physique du Solide et de Résonance Magnétique, Institut de Recherche Fondamentale, Commissariat à l'Energie Atomique-Centre d'Etudes Nucléaires Saclay, 91191 Gif-sur-Yvette Cedex, France

and

E. Paris and B. Etienne

Laboratoire de Microstructures et de Microélectronique, Centre National de la Recherche Scientifique, 92220 Bagneux, France

(Received 12 April 1988)

The existence of the magnetic-field-induced liquid-to-solid phase transition in an extreme quantum-limit 2D electron plasma is established for electrons at a high-quality GaAs/GaAlAs heterojunction by detection of a gapless magnetophonon excitation branch with radio-frequency spectroscopy. The phase diagram, determined for Wigner-Seitz to Bohr radius ratio $1.6 < r_s < 2.5$, extrapolates to a zero-temperature critical Landau-level filling factor $\nu_c = 0.23 \pm 0.04$ and a zero-filling-factor melting temperature close to the classical ($r_s \rightarrow \infty$) limit.

PACS numbers: 73.40.Kp, 64.70.-p, 73.20.Mf

A zero-temperature electron plasma confined to a plane shows unusually varied physical properties as a function of density n_s and perpendicular magnetic field H . In zero field and high density, the zero-point energy arising from the Pauli exclusion principle dominates, resulting in a liquid state with Fermi energy $E_F = \hbar^2/ma^2$, which corresponds to the energy of confinement in the Wigner-Seitz radius, a , defined by $\pi a^2 = 1/n_s$. As the density is reduced the Coulomb interaction $V_C = e^2/\epsilon a$ in the medium of dielectric constant ϵ gains in importance, ultimately ordering the electrons into a crystal. Wigner¹ predicted this quantum phase transition long ago, but it has never been seen for want of a suitable physical system.

In a magnetic field, however, each single-particle state is already confined by the Lorentz force to an area $\sim \phi_0/H = 2\pi l_H^2$ occupied by a flux quantum $\phi_0 = hc/e$ [$l_H = (\hbar c/eH)^{1/2}$ is the zero-point cyclotron radius] and takes on discrete energy values $(n + \frac{1}{2})\hbar\omega_c$ where $\hbar\omega_c = \hbar^2/ml_H^2 = \hbar eH/mc$ is the cyclotron energy. Each of these Landau cyclotron oscillators has an average share of $\nu = 2(l_H/a)^2$ electrons. Increasing the field decreases this filling factor ν , successive Landau levels empty, and, in the presence of moderate disorder, one observes the integrally quantized Hall resistance.² When $\nu < 1$ there is spatial freedom for all the electrons for the same zero-point energy. This greatly favors Coulomb-induced correlation. The many-body ground state is a correlated liquid giving rise to the fractional quantum Hall effect³ until, below a critical filling factor estimated between $\frac{1}{3}$ and $\frac{1}{9}$,⁴ a new ground state with long-range crystallike correlation is expected. To date, this transition, too, has eluded unambiguous observation.

The present experiment gives positive evidence of this magnetically induced Wigner solid.

Advances in the technology of modulation-doped

GaAs/GaAlAs heterojunctions have made available very high-quality 2D quantum electron systems. Some time ago,⁵ it was already suggested that the abnormal behavior observed in the dc transport for $\nu < \frac{1}{5}$ could be a result of a magnetically induced Wigner solid. But to be affirmative required a much more specific type of experiment.

Our experiment tests for a defining property of a solid—its rigidity to shear. An unbounded charged 2D liquid has only compressional (plasmon) excitations in zero field whose frequency-wave-vector relation is $\omega_p^2 = 2\pi e^2 n_s q/\epsilon m$. A perpendicular magnetic field introduces a gap: $\omega_{\pm}^2 = \omega_p^2 + \omega_c^2$. There are then no gapless bulk excitations.⁶ On the other hand, a system capable of resisting static shear, expressed by modulus μ , does exhibit a gapless magnetophonon branch of frequency

$$\omega_- = \omega_t^{(0)} \omega_p / \omega_c = c(2\pi\mu)^{1/2} q^{3/2} / H, \quad \omega_c \gg \omega_p, \quad (1)$$

where $\omega_t^{(0)} = (\mu/mn_s)^{1/2} q$. The presence of such a mode is taken as positive evidence of a solid phase. Such a phase will nonetheless melt at a temperature which approaches the classical melting temperature $T_{mc} = V_C/\Gamma_{mc}$ ($\Gamma_{mc} = 127 \pm 3$)⁷ as $H \rightarrow \infty$.

The experiment consists of making a longitudinal electric wave of defined wave vector q interact with the electrons and sweeping its frequency; the power transferred when $\omega = \omega_-(q)$ is detected by the diminished amplitude of the transmitted wave. About 10 pW of power from a 50–1400-MHz frequency-swept source is transmitted to a phase-compensated homodyne detector via a constant-impedance 8- μm strip meander line which exerts an electric field in the plane of the electrons, situated at height h ($\approx 3000 \text{ \AA}$) above it, described by

$$\mathbf{E} = \hat{x} \sum_p A_p \exp(-pq_0 h) \exp(ipq_0 x), \\ p \text{ integer, } q_0 = 2\pi/16 \mu\text{m}^{-1}. \quad (2)$$

TABLE I. Sample characteristics: a_i and n_i , $i=1,2$, refer to doping-plane setback distances from the heterojunction and Si donor concentrations. n_s and μ are low-temperature electron density and mobility. The structure is completed with 15 nm of GaAlAs and 5 nm of GaAs. Different thermal cycling produces a variation in n_s : For sample I, $0.5 < n_s < 1.1 \times 10^{11} \text{ cm}^{-2}$.

	a_1 (nm)	n_1 (10^{11} cm^{-2})	a_2 (nm)	n_2 (10^{11} cm^{-2})	n_s (10^{11} cm^{-2})	μ ($10^6 \text{ cm}^2 \text{ s}^{-1} \text{ V}^{-1}$)
Sample I	100	4	280	60	0.75	1.3
Sample II	75	6	135	60	1.2	1.0

As the frequency is swept, successive resonances for the sequence $q = pq_0$ are traversed, giving rise to an absorption signal which is demodulated by detection in phase with a low-frequency ($\approx 10^2 \text{ Hz}$) electric field applied between the electrons and the back of the sample. The samples were molecular-beam epitaxy grown, bilayer planar, doped GaAs:Ga_{0.68}Al_{0.32}As heterojunctions⁸ whose characteristics are given in Table I. Of overall dimensions $8 \times 4 \text{ mm}^2$, they have a mechanically etched Hall bar pattern with six diffused indium contacts, leaving the middle free for mounting face down in close contact with the meander line. The assembly is situated in the dilute phase in the plastic mixing chamber of the dilution refrigerator,⁹ coplanar with a Ru₂O₃ resistance thermometer. The field is provided by the Grenoble 50-mm bore hybrid magnet. Temperatures are estimated to be correct to 15% and fields to 0.05 T.

The results derive from six separate experiments, five on sample I recycled to 300 K. The sample is characterized at the lowest temperature ($\approx 50 \text{ mK}$) both by standard dc transport (ρ_{xx}, ρ_{xy}) at 100 nA and by simultane-

ous monitoring of the fixed-frequency (usually $\approx 100 \text{ MHz}$) absorption ($\propto \sigma_{xx}$) as a function of the field. This contactless technique allows us to observe the Shubnikov-de Haas oscillations under low power absorption (typically 1 pW) by virtue of sitting on the wing of a magnetoplasmon resonance. When $\rho_{xx}(\text{dc})$ becomes large the current is switched off to avoid excessive electron heating. The 100-MHz absorption shows typically some 30 dips for integral filling factors in addition to dips at $\nu = \frac{5}{3}, \frac{4}{3}, \frac{2}{3}, \frac{1}{3}, \frac{3}{5}, \frac{2}{5}, \frac{1}{5}$, and $\frac{3}{11}$. $\nu = \frac{4}{7}, \frac{3}{7}$, and $\frac{2}{7}$ appear in $\rho_{xx}(\text{dc})$. The rf and dc measurements for the density agree within the experimental accuracy of about 3%.

At chosen field and temperature, the 50–1400-MHz radio-frequency absorption is observed as a function of frequency. At highest field and lowest temperature, typically 28 T and 60 mK, a series of sharp resonances is seen (Fig. 1). Figure 2 shows the evolution of the spectrum for two orthogonal paths in the H - T plane. The overall behavior is similar: The well-developed sharp discrete resonances evolve towards lower frequency and broaden before disappearing. The rather abrupt disappearance of the sharp lines is accompanied by the appearance of a broad signal which disappears in its turn.

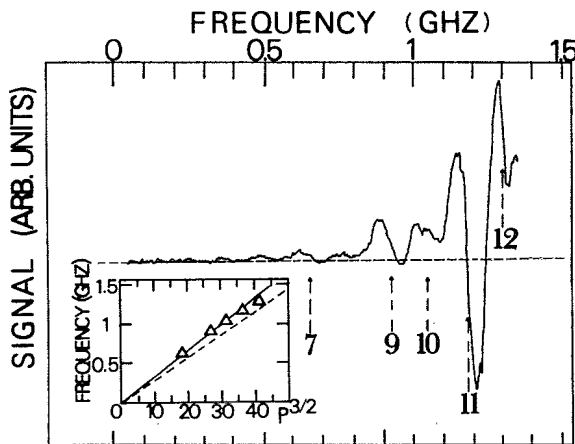


FIG. 1. Absorption spectrum at 28 T and 60 mK for density $0.77 \times 10^{11} \text{ cm}^{-2}$ (filling factor $\nu = 1/8.7$, reduced temperature $t = 0.33$) showing successive resonances and their identification as p th spatial harmonics ($q = pq_0$) of the exciting structure. The values of p are chosen for the best alignment with the origin (full line) on the accompanying plot of f_p vs $p^{3/2}$; the dashed line is the zero-order *a priori* calculation of the frequency of the lower hybrid mode of the solid.

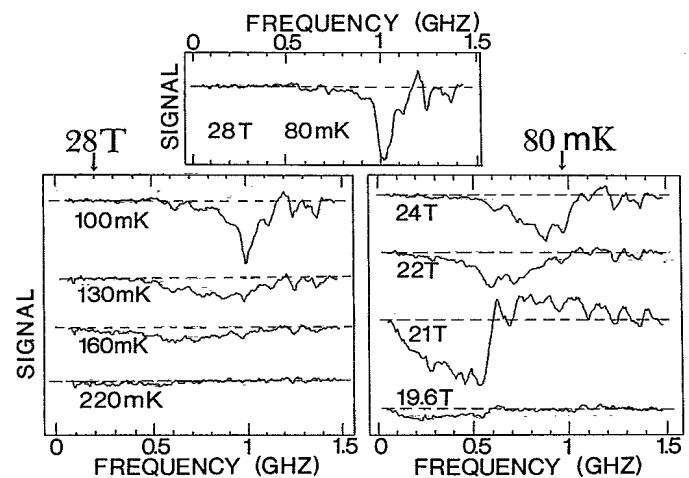


FIG. 2. Evolution of the radio-frequency absorption spectrum with temperature at constant field and with field at constant temperature. The density $n = 0.94 \times 10^{11} \text{ cm}^{-2}$. Filling factor $\nu = (3.92 \text{ T})/H$, reduced temperature $t = T/(560 \text{ mK})$.

But the detail is different: The broad signal along the constant-field path is always of the same sign, whereas for field variation it changes sign on traversing $\nu = \frac{2}{11}$ and $\frac{1}{5}$. Furthermore, there is a well-defined point in field at low temperature at which a sharp break occurs in signal as a function of field (Fig. 2: 21 T, 80 mK). Along both types of paths, the amplitude of the absorption maximum evolving from the sharp resonances shows a well-defined edge; extrapolating it to zero gives the value we associate with their appearance.

We interpret these resonances as evidence for a new phase in high field, presumably the magnetically induced Wigner solid. Their appearance defines the phase boundary of Fig. 3. The sequence of resonances is believed to arise from the lower hybrid mode of a solid phase [Eq. (1)]. Supposing the resonances to be excited by successive spatial harmonics of the meander line [Eq. (2)], we plot the resonance frequencies at 28 T, 60 mK, and $7.7 \times 10^{10} \text{ cm}^{-2}$ against the $\frac{3}{2}$ power of integers in Fig. 1. The choice of harmonics $p = 7, 9, 10, 11,$ and 12 gives a good linear alignment with the origin, whose slope is about 10% higher than an *a priori* calculation from the classical (expected for $\nu = 0$) $T = 0$ shear modulus¹⁰ and the q_0 of the line. Apart from the absence of lower harmonics, the intensities are compatible both with the expected relative variation in $q^{3/2} \times \exp(-2qh)$ ($h \approx 3000 \text{ \AA}$) and with the absolute estimate. dc transport also appears to be altered in the new phase.

Each experimental run gives the phase boundary in the H - T plane for a fixed density. Our densities correspond to $1.6 < r_s = a/a_0 < 2.5$ in units of the Bohr radius a_0 ($=100 \text{ \AA}$ for our system); this is much smaller than the critical radius for the zero-field Wigner transition,

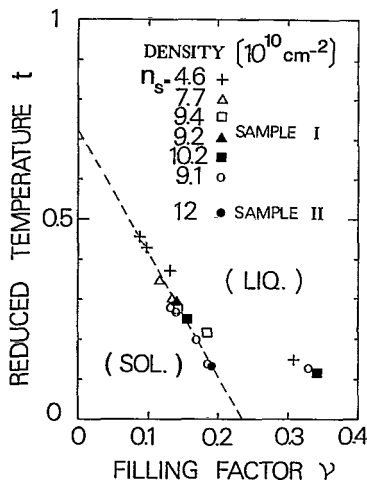


FIG. 3. Phase diagram composed from the totality of our results. The reduction for different densities is made by the employment of reduced variables $t = T/T_{mc}$ where $T_{mc} = \Gamma_{mc}^{-1} e^2/a$ is the classical melting temperature, and the Landau-level filling factor $\nu = n_s \phi_0/H$.

estimated to be $a_w = 33a_0$.¹¹ In this extreme quantum limit, where $a/a_w, l_H/a_w \ll 1$, and if only effects intrinsic to the electrons are important, all the experiments should find a common representation in terms of the reduced variables $t = T/T_{mc}$ and ν . This is done in Fig. 3. The intercepts t_c and ν_c found by extrapolation of the phase boundary to the axes should give the infinite-field melting temperature and the zero-temperature melting field. To the extent that there is no clear trend towards higher ν_c for lower density, we can represent the ensemble of the results, excluding the three outlying points, by $t/t_c + \nu/\nu_c = 1$. This has the form of a quantum Lindemann melting criterion (modified to nearest-neighbor excursion) with constant shear modulus along the melting curve. The three outlying points are clearly outside the statistical fluctuations; we have chosen to exclude them from the present analysis and to await further experiment before giving them special significance. We find thus

$$t_c = 0.72 \pm 0.1, \quad \nu_c = 0.23 \pm 0.04.$$

Correcting the Coulomb interaction for the perpendicular extension z_0 of the electron wave function¹² modifies T_{mc} to give $t_c(z_0 \rightarrow 0) = 0.87 \pm 0.15$.

Disorder seems to have a limited effect in our samples with large setback distance of the doping planes. The electrical potential from a random distribution of average density n_I of ionized donors¹³ in the doping plane produces fluctuations in the compressional strain

$$\langle \epsilon_{xx}^2 \rangle^{1/2} = C 2\pi^2 (n_I/n_S)^{1/2} (a/a_1)^3 \approx 15\%$$

with a correlation length $\sim 2a_1 \approx 2000 \text{ \AA} \approx 10a$. ($C \lesssim 1$ corrects for correlation in the ionized plane). On the other hand, the shear fluctuations $\langle \epsilon_{xy}^2 \rangle = 0$ because of the irrotational nature of the field. Our linewidths are compatible with this estimate. The density fluctuations urge caution, though, in interpreting the ρ_{xx} minima near the phase boundary, for at a given field the distribution in ν may translate into pockets of liquid (solid) in a mass of solid (liquid). Perhaps the sharp break in signal versus frequency at the transition reflects percolation of the solid phase (and of shear) across the sample. But a Coulomb system becomes more compressible as the length scale decreases, so that the short-correlation-length potential arising from impurities and defects at the interface, although less frequent, can have more disruptive effects. The residual impurity concentration in the GaAs of $\sim 10^{14} \text{ cm}^{-3}$ taken over the z extent of the electrons translates into about one pinning center for ≈ 3000 fundamental Landau states, clearly insufficient to engender a glass.¹⁴ However, line defects on the heterojunction would be very efficient at introducing strong discontinuities into the shear modulus and could be responsible for the length scale of a few microns indicated by the absence of lower spatial harmonics.

The evidence points very strongly towards the forma-

tion of a magnetically induced Wigner solid: the sequence of several discrete resonance frequencies, their q dependence, and their absolute values; the form of the phase diagram and its density dependence (fit on the t - v plot for a range of densities $0.5 < n_s < 1.2 \times 10^{11} \text{ cm}^{-2}$). There are density fluctuations, but the continuity of the solid is only interpreted on a scale of several microns.

Four of us (E.Y.A., G.D., D.C.G., and F.I.B.W.) are particularly indebted to E. Mendez and M. Heiblum for early help. We are also grateful to the Francis Bitter National Magnet Laboratory (United States) for hosting preliminary work. The inestimable technical assistance of J. Verrier, C. Chaleil, and M. Coignard is gratefully acknowledged, as are the counsel and help of P. Pari, A. Benoit, and J. L. Tholence. We are most grateful to the Centre National de la Recherche Scientifique-Max-Planck-Institut high-field magnet laboratory in Grenoble for making available the hybrid magnet, and in this respect we would like to thank in particular J. C. Vallier, J. C. Picoche, H. J. Schneider-Muntau, and G. Maret. Transatlantic collaboration was made possible by a NATO travel grant. One of us (E.Y.A.) acknowledges funding through National Science Foundation Contract No. DMR87-05-977.

^(a)Present address: Department of Physics, Rutgers University, Piscataway, NJ 08855.

¹E. P. Wigner, Phys. Rev. **46**, 1002 (1934).

²K. von Klitzing, G. Dorda, and M. Pepper, Phys. Rev. Lett. **45**, 494 (1980).

³D. C. Tsui, H. L. Stormer, and A. C. Gossard, Phys. Rev. Lett. **48**, 1559 (1982); R. B. Laughlin, Phys. Rev. Lett. **50**, 1395 (1983).

⁴J. Durkan, R. J. Elliott, and N. H. March, Rev. Mod. Phys. **40**, 812 (1968); H. Fukuyama and D. Yoshioka, J. Phys. Soc. Jpn. **48**, 1853 (1980); K. Maki and X. Zotos, Phys. Rev. B **28**, 4349 (1983); P. K. Lam and S. M. Girvin, Phys. Rev. B **30**, 473 (1984); D. Levesque, J. J. Weiss, and A. H. MacDonald, Phys. Rev. B **30**, 1056 (1984); Yu. E. Lozovik, V. M. Fartzdinov, and B. Abdullaev, J. Phys. C **18**, L807 (1985); S. T. Chui, T. M. Hakim, and K. B. Ma, Phys. Rev. B **33**, 7110 (1986); S. Kivelson, C. Kallin, D. P. Arovas, and J. P. Schrieffer, Phys. Rev. B **36**, 1620 (1987).

⁵E. Mendez, M. Heiblum, L. L. Chang, and L. Esaki, Phys. Rev. B **28**, 4886 (1983).

⁶S. M. Girvin, A. H. MacDonald, and P. M. Platzman, Phys. Rev. Lett. **54**, 581 (1985), and Phys. Rev. Lett. B **33**, 2481 (1986).

⁷C. C. Grimes and G. Adams, Phys. Rev. Lett. **42**, 795 (1979); G. Deville, J. Low Temp. Phys. **72**, 135 (1988).

⁸B. Etienne and E. Paris, J. Phys. (Paris) **48**, 2049 (1987).

⁹For which we acknowledge some design ideas and drawings from A. Benoit of the Centre de Recherche sur les Très Basses Températures, Grenoble.

¹⁰L. Bonsall and A. A. Maradudin, Phys. Rev. B **15**, 1959 (1977); K. Maki and X. Zotos, Ref. 4.

¹¹D. Ceperley, Phys. Rev. B **18**, 3126 (1978).

¹²T. Ando, A. Fowler, and F. Stern, Rev. Mod. Phys. **54**, 437 (1981), and references therein; F. C. Zhang and S. Das Sarma, Phys. Rev. B **33**, 2903 (1986).

¹³A. H. MacDonald, K. L. Liu, S. M. Girvin, and P. M. Platzman, Phys. Rev. B **33**, 4014 (1986).

¹⁴H. Aoki, J. Phys. C **12**, 633 (1979).